Pore dimensions and the role of occupancy in unitary conductance of Shaker K channels

Ignacio Díaz-Franulic,[1,2] Romina V. Sepúlveda,[3] Nieves Navarro-Quezada,[1] Fernando González-Nilo,[1,3] and David Naranjo[1]

[1]Centro Interdisciplinario de Neurociencia de Valparaíso and [2]Programa de Doctorado en Ciencias mención Neurociencia, Universidad de Valparaíso, Valparaíso 2360103, Chile
[3]Center for Bioinformatics and Integrative Biology, Universidad Andrés Bello, Santiago 8370146, Chile

K channels mediate the selective passage of K^+ across the plasma membrane by means of intimate interactions with ions at the pore selectivity filter located near the external face. Despite high conservation of the selectivity filter, the K^+ transport properties of different K channels vary widely, with the unitary conductance spanning a range of over two orders of magnitude. Mutation of Pro475, a residue located at the cytoplasmic entrance of the pore of the small-intermediate conductance K channel Shaker (Pro475Asp (P475D) or Pro475Gln (P475Q)), increases Shaker's reported ∼20-pS conductance by approximately six- and approximately threefold, respectively, without any detectable effect on its selectivity. These findings suggest that the structural determinants underlying the diversity of K channel conductance are distinct from the selectivity filter, making P475D and P475Q excellent probes to identify key determinants of the K channel unitary conductance. By measuring diffusion-limited unitary outward currents after unilateral addition of 2 M sucrose to the internal solution to increase its viscosity, we estimated a pore internal radius of capture of ∼0.82 Å for all three Shaker variants (wild type, P475D, and P475Q). This estimate is consistent with the internal entrance of the Kv1.2/2.1 structure if the effective radius of hydrated K^+ is set to ∼4 Å. Unilateral exposure to sucrose allowed us to estimate the internal and external access resistances together with that of the inner pore. We determined that Shaker resistance resides mainly in the inner cavity, whereas only ∼8% resides in the selectivity filter. To reduce the inner resistance, we introduced additional aspartate residues into the internal vestibule to favor ion occupancy. No aspartate addition raised the maximum unitary conductance, measured at saturating [K^+], beyond that of P475D, suggesting an ∼200-pS conductance ceiling for Shaker. This value is approximately one third of the maximum conductance of the large conductance K (BK) channel (the K channel of highest conductance), reducing the energy gap between their K^+ transport rates to ∼1 kT. Thus, although Shaker's pore sustains ion translocation as the BK channel's does, higher energetic costs of ion stabilization or higher friction with the ion's rigid hydration cage in its narrower aqueous cavity may entail higher resistance.

INTRODUCTION

K channels elicit the passage of K^+ across the hydrophobic core of the membrane, with high transport rates and exquisite discrimination among cations having similar ionic radii and valence (Parsegian, 1969; Harris et al., 1998; Hille, 2001; Zhou et al., 2001; Long et al., 2005). This property appears to rise from a key feature common to members of the K channel family: the "signature sequence" of eight amino acidic residues (TMxTVGYG) forming the narrowest section of the conduction pathway. As proposed in the early 1970s and confirmed by crystallographic data in 2001, the oxygen atoms of carbonyl groups of what we know now as the "selectivity filter" coordinate the incoming K^+, acting as water surrogates, lowering the energetic cost to place a partially dehydrated ion within the membrane realms (Bezanilla and Armstrong, 1972; Heginbotham et al., 1994; Zhou et al., 2001; but see Yu et al., 2010). Considering the high degree of conservation of the signature sequence, it is surprising to find that single-channel conductance displays wide variability among K channels, which ranges between 2 and 250 pS in standard experimental conditions (around 100 mM of symmetric potassium). Such dispersion gives rise to the general division between small and large conductance K (BK) channels (Latorre and Miller, 1983; Blatz and Magleby, 1986; Carvacho et al., 2008; Moscoso et al., 2012).

Electrostatic calculations on MthK, a large conductance open bacterial K channel structure (Protein Data Bank [PDB] accession no. 1LNQ), showed that the transpore electric field is highly focused along the selectivity filter (Jiang et al., 2002). Thus, ion transit across this narrow region is expected to be the rate-limiting steps for K^+ translocation. In addition, the voltage-dependent Ag^+ accessibility to the CNG channel pore indicates that

Correspondence to David Naranjo: david.naranjo@uv.cl
Abbreviation used in this paper: BK, large conductance K.

The Rockefeller University Press $30.00
J. Gen. Physiol. Vol. 146 No. 2 133–146
www.jgp.org/cgi/doi/10.1085/jgp.201411353

most of the electric field drops along its selectivity filter (Contreras et al., 2010). However, theoretical studies predicted that as the pore cavity sectional area increases, the required energy for a potassium ion to dwell inside gets smaller by 4–28 kcal × mol^{-1} per $Å^{-1}$ in the pore radius (Parsegian, 1969; Chung et al., 2002; Jogini and Roux, 2005; Treptow and Tarek, 2006). Then, because the cavity diameter in the structure of the Kv1.2/2.1 chimera (PDB accession no. 2R9R) is ∼10 Å narrower than that of the MthK channel, a common structural template for BK channels, it should be energetically more expensive to put an ion in the Kv cavity, decreasing the ion transport rate. Thus, in narrow channels a significant part of the electric field may drop in the cavity.

With a reported unitary conductance of ∼20–25 pS at 100–150 mM and ∼45 pS at saturating symmetrical K^+ (Heginbotham and MacKinnon, 1993), the voltage-gated Shaker K channel is a small-intermediate conductance K channel. We have proposed that, unlike large conductance channels, the rate-limiting step for ion conduction in this channel is not ion translocation across, but the movement toward or from, the selectivity filter (Moscoso et al., 2012). In Shaker, most of the electrical resistance would be located outside the selectivity filter. Then, the electric field would not be as focused across that structure as in BK channels, but more spread out along the whole pore. Thus, a single-point mutation, Pro475Asp, in the PVP region at the Shaker internal entrance increases unitary conductance to ∼100 pS in 100 mM K^+ and to ∼200 pS at saturating K^+ (Sukhareva et al., 2003; Moscoso et al., 2012). This latter conductance is only one third of BK channel's ∼600-pS maximum conductance (Eisenman et al., 1986; Brelidze et al., 2003), narrowing the gap between the overall energy of K^+ transport rates between Shaker and BK channels to ∼1 kT units. It seems that P475D channels' large conductance is achieved by increasing pore occupancy with the addition of new K^+-binding sites (Moscoso et al., 2012).

In this paper, we probe Shaker internal entrance dimensions and the contribution of separate zones of the pore to the overall resistance. To do so, we unilaterally applied high sugar concentration to increase the solution viscosity either internally or externally. To test the influence of pore occupancy in single-channel conductance, we constructed variants with additional aspartate residues in the internal vestibule of Shaker-WT and P475D to further raise K^+ density along the pore, and measured their unitary conductance in a wide range of K^+ concentrations.

MATERIALS AND METHODS

Channel expression and patch-clamp recordings of Shaker K channels

All Shaker mutants were generated with the QuickChange site-directed mutagenesis kit (Agilent Technologies). For transcription, pBlu-SK plasmids containing Shaker-IR were linearized with NotI and incubated with T7 mMESSAGE Machine kit (Applied Biosystems). cRNA was suspended in 15 µl water and stored at −80°C. *Xenopus laevis* oocytes were injected with 0.1–1.0 ng cRNA and recorded 24–48 h later with the patch-clamp technique. Patch pipettes were made from borosilicate glass (World Precision Instruments) with the tip fire-polished to resistances of 2–60 MΩ. Electrodes and bath contained the experimental recording solutions of potassium methanesulfonate or KCl, plus 5 mM EGTA, 2 mM KCl, and 10 mM HEPES, pH 7.4. All experiments were done in the inside-out configuration, except for those in high external sucrose, which were made in outside-out patches (Fig. S3). For measurements in high solution viscosity, after checking for the presence of one to two channels in the patch, the bath solution was perfused with a volume equivalent to fivefold the volume of the recording chamber, with a solution containing an additional 2 M sucrose.

Voltage commands and current recordings were performed with an Axopatch 200B amplifier through a Digidata 1200B or Digidata 1440 interface with pClamp 8 or pClamp 10 suites (Molecular Devices). Current traces were Bessel filtered to 5 kHz and acquired at 100 kHz. Individual traces were digitally refiltered to 1–2 kHz for analysis. I-V relations were built by averaging the amplitude of open events >10 ms from 5–10 leak-subtracted single-channel traces from each experiment. These I-V relations were fitted to a third-degree polynomial function to allow for concave and convex shapes in the I-V relations. The derivative at zero voltage was used to calculate unitary conductance. The conductance versus $[K^+]$ relations were fitted to a Langmuir isotherm, which describes the data with two parameters: the dissociation constant and g_{max}, the maximum conductance. g_{max} could be unambiguously estimated by measuring conductances in a wide range of $[K^+]$ (Eisenman et al., 1986; MacKinnon and Miller, 1989; Naranjo and Latorre, 1993). Results are expressed as mean ± SEM, with n, the number of patches, between 3 and 5, unless stated otherwise.

Molecular dynamics simulations

Based on the homology model published by Moscoso et al. (2012), eight molecular systems of Shaker were built: WT, A471D, V476D, P475D, S479D, P475D/V476D, P475D/S479D, and A471D/P475D/S479D. In the first place, each Shaker structure was oriented to the z axis and embedded into a membrane composed by phosphatidyloleoyl phosphatidylcholine lipids. The force field CHARMM36 united-atom was defined for the membrane lipids (Hénin et al., 2008), and the CHARMM27 force field with the CMAP correction was defined for proteins (MacKerell et al., 1998, 2004). Every system was hydrated by adding a water box with water molecule type TIP3P (Jorgensen et al., 1983) and, subsequently, ionized at 500 mM KCl. The total dimensions of the systems was 160 × 160 × 180 Å.

The initial conformations of each system were minimized in 50,000 steps and equilibrated by means of molecular dynamics of 2 ns with the α carbons restrained. The molecular dynamics simulations were executed with NAMD 2.9 software (Phillips et al., 2005), and the data production for each system were obtained above 10 ns. A constant temperature (300°K)/constant pressure (1 Atm) ensemble was used for all molecular dynamics. The pressure was fixed with the Langevin piston method, and the temperature was controlled using Langevin dynamics with a damping coefficient of 1 ps^{-1} (Feller et al., 1995). Periodic boundary conditions were set, and the Ewald method was used to calculate the long-range electrostatic interactions into a grid-spacing <1 Å. Restraints of 0.5 kcal mol^{-1} $Å^{-2}$ were applied to the secondary structure α carbons.

Estimation of K^+ ion hydrodynamic radius

We developed a method to estimate the hydrodynamic radius of potassium ions by using our own measures of the internal radius of capture of the Shaker pore (Fig. 1) together with the structure of the Kv1.2/2.1 paddle chimera channel (PDB accession no.

2R9R; Long et al., 2007). The rationale consists of (a) to calculate the molecular surface of the internal entrance of the channel with a sphere of variable radius rolled on top of the van der Waals surface of the exposed residues (Richards, 1977), and (b) to calculate the capture radius for K^+ by taking the difference between the effective pore radius left by the rolling sphere and the radius of the probe (the putative hydrated K^+). When such difference matches the experimentally obtained capture radius in diffusion-limited measures, as in Fig. 1, the radius of the probe becomes an estimate for the hydrodynamic radius of the approaching K^+ ions.

Consider the cross section of a pore in Fig. S1. Like many porous structures, the effective pore size radius is equal to the radius of the largest sphere that is able to pass (Ferry, 1936). Thus, the pore opening is determined by the effective size of the K^+ ion (or the spherical probe) that, in turn, depends on the average number of water molecules forming its hydration shell. If K^+ is a point charge (no physical dimension and no hydration shell) and the protein is a rigid structure, the effective pore opening to pass will be specified by the van der Waals envelope of the pore walls (Fig. S1 A; Richards, 1977). But, if instead, K^+ is a solid body of finite dimensions, it will not be able to pass across a surface tortuosity smaller than its own size, reducing the sectional area available for permeation (Fig. S1, B–E). On the other extreme, if K^+ is a sphere with a radius larger or identical to the effective radius of the pore, it will not be able to permeate (Fig. S1 F). For each case, we draw the largest circle to circumscribe—and the smallest circle to inscribe—the pore, with radii named r_{min} and r_{max}, respectively. The effective opening should be somewhere in between these estimates (Fig. S1, B–E). Because of the loss in surface tortuosity, one expected result in radially symmetric structures is that r_{max} and r_{min} converge to the same value when the probe size reaches the effective pore size.

We represented the structure of the paddle chimera channel Kv1.2/2.1 in a VMD environment (http://www.ks.uiuc.edu; Humphrey et al., 1996). The surface of the channel structure was calculated in the surf representation with an increasingly larger rolling probe onto the protein surface (Graphics/Representations/Drawing Method/Surf). We varied the probe radius (r_P) between 1.3 and 4.6 Å, i.e., from a sphere of about the size of a naked K^+ to one too big to get inside the pore. In the surf representation, for larger radii spheres ($r_P > 4.6$ Å) the pore becomes just another dimple on the protein's surface. The magnitudes r_{max} and r_{min} were measured with a ruler on top of a 1-Å grid directly on the screen (Extensions/Visualization/Ruler/grid) (Fig. S1, B–E). Thus, the differences: $r_{max} - r_P$ or $r_{min} - r_P$ should be equivalent to the maximum or minimum capture radius of the pore, respectively (Fig. 6 G).

Online supplemental material

Fig. S1 shows the methodology used to estimate the hydrodynamic radius of the K^+ ion. Fig. S2 shows representative inward current traces of outside-out patches in the absence and presence of 2 M of external sucrose to measure the external access resistance. Fig. S3 shows individual measurements of cationic selectivity by determination of the bi-ionic potentials after replacement of internal K^+ in inside-out patches. Fig. S4 shows that aspartate addition at position 476 in a background of P475Q does not decrease the maximum K^+ unitary conductance in Shaker P475Q channels. The online supplemental material is available at http://www.jgp.org/cgi/content/full/jgp.201411353/DC1.

RESULTS

Diffusion-limited currents in Shaker K channels suggest a narrow internal pore entrance

As Brelidze and Magleby (2005) did for BK channels, we measured the diffusion-limited unitary outward currents of Shaker variants in a highly viscous solution to obtain functional estimations for their internal entrance dimensions. At high positive voltage, the unitary outward current amplitude asymptotically approaches to a diffusion-limited, voltage-independent regime. This amplitude allows us to estimate the average capture radius of the channel pore (Läuger, 1976; Andersen and Procopio, 1980; Andersen, 1983; Brelidze and Magleby, 2005). Considering a hemispheric internal access to the pore, the maximum diffusion-limited unitary current i_{DL} is:

$$i_{DL} = 2\pi z e_o r_c D c, \quad (1)$$

where z is the valence of the permeant ion, e_o is the elementary charge, c is the bulk concentration of K^+, and D is its diffusion coefficient. If we assume K^+ as a point charge, r_C represents the radius of the pore entrance (Andersen, 1983; Brelidze and Magleby, 2005). However, ions are supposed to have finite sizes; thus, we have to assume a physical radius for the ion to be able to estimate the physical dimension of the pore. If we assume that ions are solid spheres with radius r_I entering a circular pore opening of radius r_O, then $r_C = r_O - r_I$ (Ferry, 1936; Andersen, 1983; Brelidze and Magleby, 2005). The rationale for this subtraction is based on the fact that the total number of effective collisions for either the point or the finite charge will not change for identical radial deviations from the central trajectory.

We set out to measure diffusion-limited outward currents of Shaker-WT and P475D in the presence of 2 M sucrose in which the effective D is ~0.14 of the control solution (Brelidze and Magleby, 2005). But, to compare measurements between these two variants, it is necessary to take into consideration some features of the P475D mutation: (a) the α-helical bending role of proline residues (Wilman et al., 2014), with the possible structural changes associated with the P475D mutation; (b) its deep impact on channel activation properties (Sukhareva et al., 2003); and (c) the fact that Eq. 1 assumes that the entrance is not charged, thus the local K^+ concentration in the P475D pore entrance is surely different from that of the bulk solution. To assess the extent of the changes to the internal entrance dimensions produced by the replacement of Pro475, we also measured the diffusion-limited currents of P475Q because it is a neutral proline replacement that produced an already known increment of three- to fourfold in the unitary conductance (Sukhareva et al., 2003). Fig. 1 shows leak-subtracted, single-channel traces of Shaker-WT (A), P475Q (B), and P475D (C) in 100 mM of symmetrical KCl and with 2 M sucrose added to the internal side. With sucrose, the unitary currents of Shaker-WT and P475Q appear to become voltage independent at V > 220 mV, reaching values of 1.25 ± 0.032 pA (average current between 260 and 380 mV) and 1.22 ± 0.045 pA

(average current between 220 and 300 mV), respectively. Thus, apparently the Pro475Gln mutation does not change significantly the dimensions of the internal entrance (P = 0.25 of a two-tail *t* test). On the other hand, for P475D, the voltage-independent current had an amplitude of 2.40 ± 0.27 pA, about twice the size of that of Shaker-WT (Fig. 1 C). Because (a) P475D outward currents are reduced to 50% after doubling the internal ionic strength with NMDG-Cl with respect to an equivalent osmolarity increment with sucrose (Moscoso et al., 2012), and (b) Eq. 1 predicts a linear relationship between limiting current and $[K^+]$, we postulate that the carboxyl group of 475 side chains is doubling the local K^+ concentration. Collectively, these values suggest that the internal entrance in all three variants, WT, P475Q, and P475D, has similar dimensions.

Assuming an effective diffusion coefficient for K^+ of 0.25×10^{-5} cm^2 s^{-1} in a solution having 100 mM KCl and 2 M sucrose (Brelidze and Magleby, 2005), from Eq. 1 we estimate r_C = 0.82 ± 0.02 Å and r_C = 0.84 ± 0.03 Å for Shaker-WT and P475Q channels, respectively. Considering that r_C is the difference between the radius of the ion and the channel entrance, and that K^+ ions access the conduction pathway, preserving their hydration sphere, 3.6–6.6 Å needs to be added to our estimates to account for the internal entrance radial dimensions (Andersen and Procopio, 1980; Andersen, 1983; Enderby, 1995; Zhou et al., 2001). We used our estimated capture

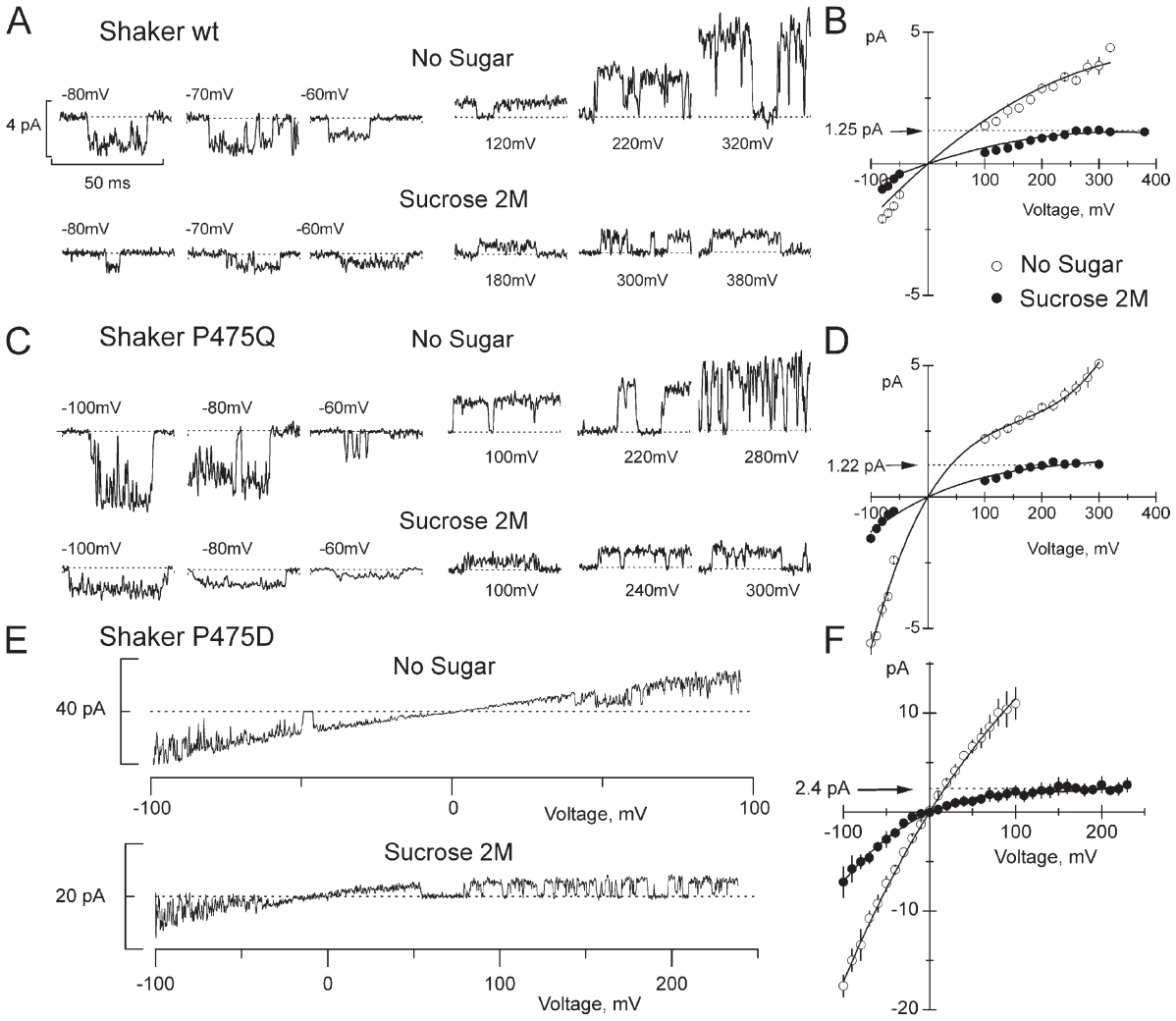

Figure 1. Diffusion-limited currents of Shaker K channels. (A, C, and E) Single-channel current traces of Shaker variants in 100 mM of symmetrical KCl (top) and with 100 mM KCl plus 2 M sucrose in the bath (bottom). (A) Shaker-WT, (C) P475Q, and (E) P475D. (B, D, and F) Open-channel I-V relations of at least five traces from two to four independent experiments. (B) Shaker-WT, (D) P475Q, and (F) P475D. Open and closed symbols correspond to control and sucrose data points, respectively. The solid lines are fits of a third-degree polynomial function with no theoretical meaning. The last four points taken at the most positive voltage of each curve were averaged to obtain the diffusion-limited current value for each data series. Shaker-WT, i_{DL} = 1.25 ± 0.032 pA; P475Q, i_{DL} = 1.22 ± 0.045 pA; P475D, i_{DL} = 2.40 ± 0.27 pA.

radius for Shaker-WT to assess the size of the K^+ hydrodynamic radius by comparing it with the pore opening left on the Kv1.2/2.1 channel structure (PDB accession no. 2R9R). The rationale required calculating the molecular surface of the internal entrance left by a sphere of variable radius rolled on top of the van der Waals surface of the exposed residues (see details in Materials and methods) (Richards, 1977). Then, we calculated the capture radius for the probe (the putative hydrated K^+) by taking the difference between the effective pore radius left by the rolling sphere radius and its own radius. When such a difference matched 0.82 Å, the experimentally obtained capture radius in our diffusion-limited measurements (Fig. 1), the radius of the probe became an estimate for the hydrodynamic radius of approaching K^+ ions. This match occurred when the radius of the probe was set to 3.8–4.1 Å (See Fig. 6 and Discussion).

Estimation of Shaker's internal and external access resistances

In all three Shaker variants, internal sucrose also decreased the amplitude of unitary inward currents (Fig. 1). We used these decrements to estimate the contribution of the internal access resistance to the overall channel resistance under the assumption that sucrose did not access the permeation pathway. The total resistance, R_T, is the contribution of the pore resistance (R_P) and the access resistance (R_{AccIn}): $R_T = R_P + R_{AccIn}$. We defined R_{TSuc} as the total resistance in 2 M sucrose. This resistance is larger than R_T because of a 7.14-fold increment in the resistivity of the intracellular solution (Brelidze and Magleby, 2005). Thus, the total increment in resistance is $R_{TSuc} - R_T = 7.14\ R_{AccIn} - R_{AccIn}$, and then:

$$R_{AccIn} = \frac{R_{Tsuc} - R_T}{6.14}. \quad (2)$$

In a similar fashion, we could estimate the external access resistance, R_{AccEx}, with the addition of 2 M sucrose to the external solution in outside-out patches (Fig. S2). Table 1 summarizes the estimated zero-voltage resistance measured for the Shaker variants in the presence of 2 M sucrose on either side of the channel and the estimated internal and external access resistances. By separating the contribution of both the internal and external access resistances (R_{AccIn} and R_{AccEx}) from the total resistance at 100 mM K^+, we also estimated the inner pore resistance ($R_{InnerPore}$), a portion of the pore, including the selectivity filter, where sucrose cannot reach. The external access resistance is about the same for all variants, indicating similar external geometry and charge environment that, given that it is a mutation-free zone, validates this strategy. On the other hand, the internal access resistance for Shaker-WT and P475Q is near 9 GΩ, whereas it was 1.5 GΩ for P475D. If the effective radius of capture of P475D is twice that of the uncharged variants, as Fig. 1 shows, this difference is threefold greater than expected. Such discrepancy may be caused by dissimilar sucrose invasion into the pore in the different variants (See Discussion).

The inner pore resistance is 3.0 GΩ for P475D and 3- and 10-fold higher, respectively, for P475Q and Shaker-WT. Then, we may consider 3.0 GΩ as the upper limit for the resistance of P475D's selectivity filter. Because the selectivity properties of the filter in all tested Shaker variants remained unchanged, as suggested by nearly identical permeability ratio sequences (Fig. S3), their selectivity filter resistance should be similar. Thus, the internal part of the cavity of P475Q and Shaker-WT should have resistances of ∼6 and ∼27 GΩ, respectively.

Introduction of negative charged rings to the internal entrance of Shaker-WT increases local [K^+]

We introduced negative charges along the Shaker pore to test to what extent the increment in occupancy would reduce pore resistance. First, we added negatively charged rings similar to those existing at the internal entrance of BK channels. In BK channels, two glutamate residues per subunit raise the outward unitary conductance by increasing the local internal K^+ concentration (Brelidze et al., 2003). We introduced negatively charged rings at positions 476 and 479 to Shaker (corresponding to MSlo Glu321 and Glu324, respectively) to assess their contribution to conductance. Fig. 2 summarizes the effect of the charged rings on Shaker unitary conductance measured in different symmetrical potassium methanesulfonate concentrations. We measured Shaker-WT conductance in the 100–3,000-mM K^+ interval (Fig. 2 A),

TABLE 1

Effect of internal or external sucrose additions on pore resistances

Variant	R_T (Control)	R_{TSuc} (Int. sucrose)	R_{TSuc} (Ext. sucrose)	R_{AccIn}	R_{AccEx}	$R_{InnerPore}$
WT	39 ± 1	90 ± 5	53 ± 2	8.2 ± 0.7	2.1 ± 0.4	30 ± 1
P475Q	20 ± 2	77 ± 7	31 ± 1	9.3 ± 1.1	1.5 ± 0.3	9.3 ± 1.0
P475D	6.6 ± 0.2	16 ± 1	19 ± 1	1.5 ± 0.5	2.0 ± 0.1	3.0 ± 0.3

R_T is the resistance measured in 100 mM of symmetric K^+. R_{TSuc} was measured with 2 M sucrose added unilaterally to either the internal or external side. Resistances were measured by estimating the slope conductance crossing the plot's origin as in Figs. 1 and S2. R_{AccIn} and R_{AccEx} are the access resistances of the internal and external entrances, respectively, whereas $R_{InnerPore}$ is the resistance of the pore region that is not sucrose accessible. R_{AccIn}, R_{AccEx}, and $R_{InnerPore}$ were calculated from Eq. 2, assuming a 7.14-fold increment in the resistivity of the solution after the addition of 2 M sucrose (Brelidze and Magleby, 2005). All estimations are from a minimum of three individual patches. Resistances are in GΩ.

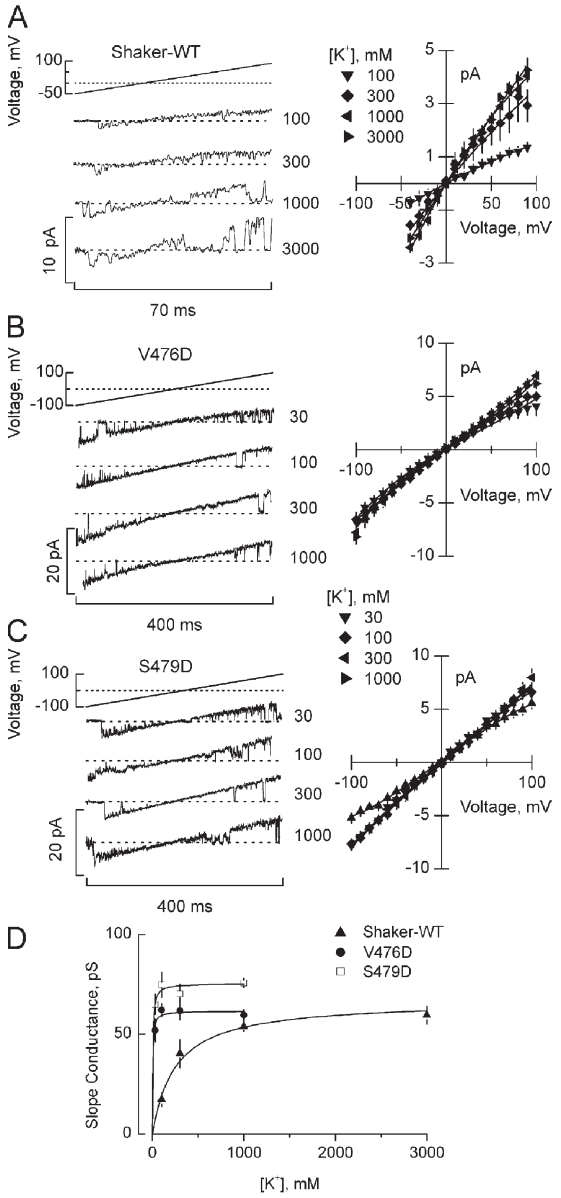

Figure 2. Effect of introducing charged residues at the internal entrance of Shaker-WT channels. (Left) Leak- and capacitance-subtracted single-channel traces of (A) Shaker-WT, (B) V476D, and (C) S479D in a wide range of symmetrical $[K^+]$ (100–3,000 mM for Shaker-WT and 30–1,000 mM for V476D and Shaker-S479D). (Right) I-V relations obtained from open-channel amplitudes. Data correspond to $n \geq 10$ traces from three separated patches. Data were fitted by a third-degree polynomial function having no theoretical meaning, and the slope of the fit traces at zero voltage was used to obtain the conductance values. (D) Zero-voltage slope conductance of the unitary currents displayed in the right panels of A–C. Data were fitted to a Langmuir isotherm for comparative purposes. Fit parameters: Shaker-WT, Kd = 250 ± 38 mM and g_{max} = 59 ± 10 pS; V476D, Kd = 3.6 ± 2.6 mM and g_{max} = 61 ± 3 pS; S479D, Kd = 4.7 ± 1.6 mM and g_{max} = 75 ± 3 pS. The discrepancy with the maximum conductance of ∼45 pS measured for Shaker-WT (Heginbotham and MacKinnon, 1993) is possibly caused by the absence of added Mg^{2+} in our solutions. Mg^{2+} could induce a low affinity blockade that reduces single-channel conductance (Heginbotham and MacKinnon, 1993; Harris et al., 1998; Moscoso et al., 2012).

whereas we used 30–1,000 mM K^+ for V476D and S479D (Fig. 2, B and C). On the left side of the figure are leak- and capacitance-subtracted representative unitary current traces elicited by voltage ramps, whereas on the right side are the I-V relations obtained from the open-channel amplitude. Unitary conductances that were calculated from the slope at 0 mV (see Materials and methods) are plotted in Fig. 2 D. As in BK and KcsA channels, the negatively charged rings at the internal entrance produced a dramatic increase of single-channel conductance at 100 mM K^+; in this case, it was a four- to fivefold increment. At higher K^+ concentrations, the increase is far

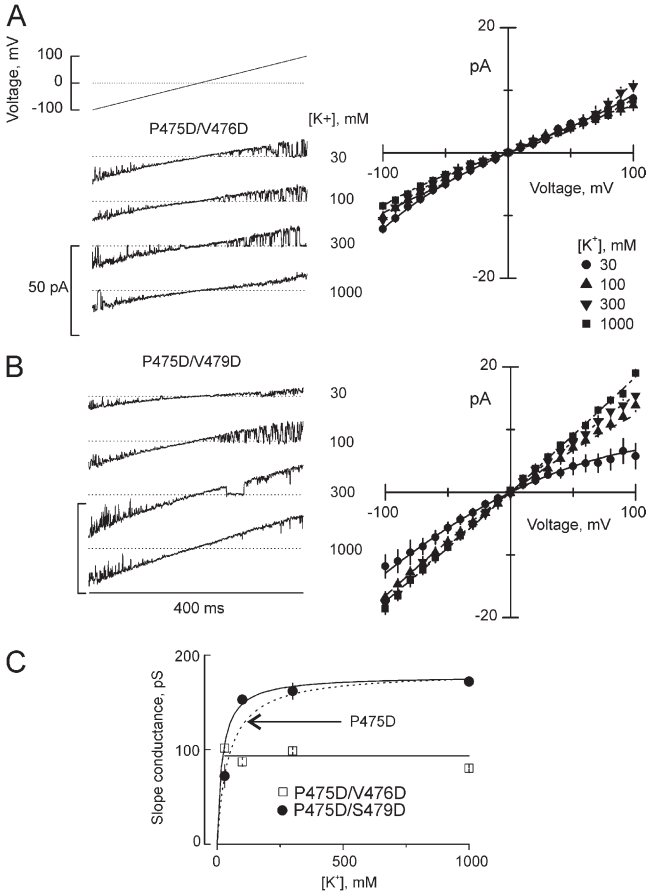

Figure 3. Effect of introducing charged residues at the internal entrance of P475D channels. (Left) Leak- and capacitance-subtracted single-channel traces of (A) P475D/V476D and (B) P475D/S479D in the 30-1,000-mM range of symmetrical $[K^+]$. (Right) I-V relations from the unitary amplitudes of both variants. The slope third-order polynomial fits were used to obtain the conductance values at zero voltage. (C) Zero-voltage slope unitary conductance obtained from the I-V relations displayed in A and B plotted versus $[K^+]$. Data of P475D/S479D were fitted to a Langmuir isotherm (Kd = 22 ± 7 mM and g_{max} = 179 ± 10 pS), whereas the data of P475D/V476D could not be fitted by a Langmuir isotherm; instead, we choose to average the unitary conductance of the channel at all K^+ concentrations (g_{max} = 87 ± 1 pS). For better comparison, we included the fit of P475D from Moscoso et al. (2012) (Kd = 48 ± 6 mM and g_{max} = 186 ± 2 pS; discontinued line).

less drastic or even negligible, as indicated by the attempts to fit to a Langmuir hyperbola used to assess the maximum conductances (g_{max}), which were: 59 ± 10 pS (n = 3), 61 ± 3 pS (n = 3), and 75 ± 3 pS (n = 3) for Shaker-WT, V476D, and S479D, respectively (continuous lines in Fig. 2 D). Thus, as in BK and KcsA channels, at lower K^+ concentrations the charged ring may electrostatically attract K^+ in the vicinity of the internal channel entrance, but at higher K^+ the electrostatic potential is strongly screened by the higher ionic strength, decreasing the K^+ excess (Brelidze et al., 2003; Nimigean et al., 2003). In summary, these results suggest that residues 476 and 479 in Shaker, when charged, work as they do in BK and KcsA channels.

We next tested for the charged rings' influence on current amplitude of the large conductance P475D variant (with g_{max} = 186 pS; Sukhareva et al., 2003; Moscoso et al., 2012). In the 30–1,000-mM [K^+] range, P475D/V476D and P475D/S479D responded very differently to K^+ (Fig. 3, A and B). Although P475D/S479D showed similar K^+ dependence as P475D (dashed line in Fig. 3 C), P475D/V476D unitary conductance was virtually K^+ independent but with maximum conductance ∼50% of that of P475D (g_{max} = 87 ± 1 pS; open symbols). On the contrary, the P475D/S479D maximum conductance is very similar to that of P475D with g_{max} = 179 ± 10 pS (n = 3; closed symbols). These results indicated that as in Shaker-WT (Fig. 2), KcsA, and BK channels, the ring at 479 raises local K^+ concentration (Brelidze et al., 2003; Nimigean et al., 2003). However, it is somehow unexpected that the negatively charged ring at 476 produced a 50% reduced maximum conductance with respect to P475D. Such reduction seems to be specific for the presence of an aspartate at position 475 because the P475Q/V476D variant showed maximum unitary currents similar to P475Q (Fig. S4). In fact, the [K^+] dependence of the P475Q/V476D variant is qualitatively and quantitatively similar to that of V476D on top of a WT background. On the other hand, the reduced maximum conductance of P475D/V476D is not consistent with a simple inhibition mechanism by a contaminant ionic compound present in the recording solution because that would not maintain the same percentage of inhibition along more than one order of magnitude of K^+ concentration and ionic strength. We do not have an explanation for this phenomenon. The lack of K^+ dependence may represent the behavior of a saturated pore in which the double charged ring characteristic of P475D/V476D acts as an electrostatic trap for K^+ ions, decreasing by 50% their rate of exit in any direction.

Addition of negatively charged residues at the inner cavity increased pore occupancy but did not raise the maximum conductance

We tested the effect of increasing the pore occupancy by the introduction of negatively charged residues proximal to 475, within the internal vestibule. Simplistically speaking, if solvent-exposed, these additional negative charges oriented into the pore would make more K^+-binding sites to be filled, favoring a knock-on mechanism (Miller, 2001; Moscoso et al., 2012). Similar to expression patterns reported for substitutions proximal to P475 by Hackos et al. (2002), charge additions between 470 and 474, except for A471D, resulted in nonfunctional or non-expressed protein. Thus, residue 471 in Shaker is not buried in the protein as indicated in the structure of the Kv1.2/2.1 chimera (see Fig. 5 A). A471D showed g_{max} ∼50% larger than that of Shaker-WT,

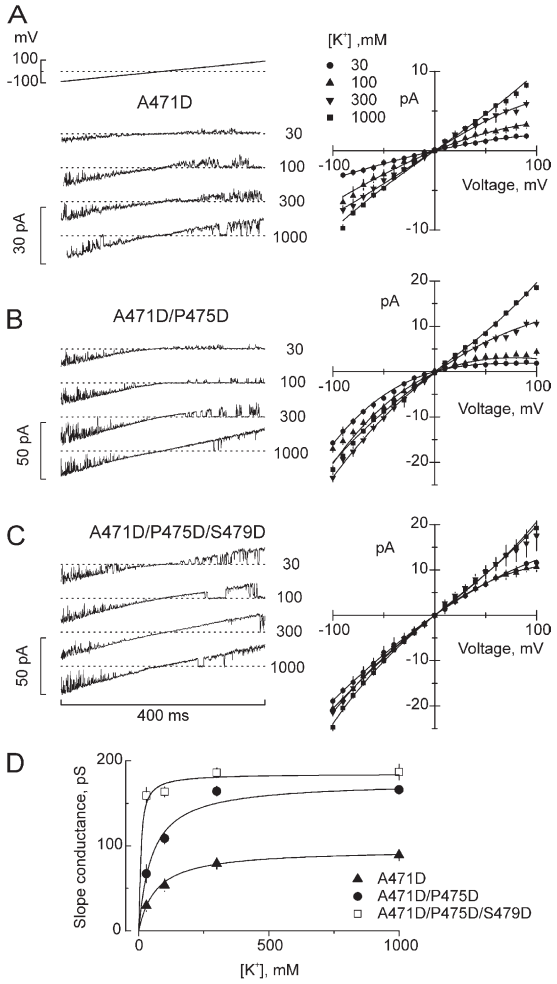

Figure 4. Charge additions at the inner cavity of Shaker K channels. (Left) Leak- and capacitance-subtracted single-channel traces of (A) Shaker-A471D, (B) P475D/A471D, and (C) P475D/S479D/A471D in the 30-1,000-mM range of symmetrical [K^+]. (Right) I-V relations obtained from open-channel amplitudes. The continuous traces are third-degree polynomial functions fitted to the data. The slope of the fit function at zero voltage was used to obtain the conductance values. (D) Slope conductance of open-channel amplitude displayed in A–C is plotted vs. [K^+]. Data were fitted to a Langmuir isotherm with the following fitting parameters: A471D, Kd = 67 ± 1.4 mM and g_{max} = 96 ± 2 pS; P475D/A471D, Kd = 65 ± 12 mM and g_{max} = 175 ± 4 pS; P475D/S479D/A471D, Kd = 6.7 ± 3.3 mM and g_{max} = 185 ± 6 pS.

suggesting that the mutation A471D may indeed increase pore occupancy in a WT background (g_{max} = 96 ± 2 pS; closed triangles in Fig. 4 D). Meanwhile, the substitution A471D/P457D and A471D/P475D/S479D reached g_{max} = 175 ± 4 pS and g_{max} =185 ± 6 pS, respectively, very similar to P475D alone.

To test if pore occupancy was increased in these mutants, we perform equilibrium molecular dynamics simulations of the three mutants described in Fig. 4 and Shaker-WT (See Materials and methods). We built structures for the open WT and the charged variants used here by comparative modeling with the pore domain of Kv1.2 (PDB accession no. 2A79; Moscoso et al., 2012). The protein models were embedded in a hydrated phosphatidyloleoyl phosphatidylcholine lipid bilayer, and K^+ ions were added to reach 500 mM, a concentration in which the conductance of most of our variants is nearly maximal. As an index of pore occupancy, K^+ densities were calculated in 0.5-Å slices along a 5-Å radius cylinder concentric with the pore (Moscoso et al., 2012) (Fig. 5 A). Fig. 5 B shows similar ion densities at the selectivity filter for all variants but differed greatly toward the internal entrance. In contrast to Shaker-WT, A471D showed two peaks near the center of the cavity indicating increased K^+ occupancy. This higher ion density is clearly associated with the Asp471 side chain, suggesting, as expected from the experimental data, an overall increment in pore occupancy. Further increments over P475D are observed with the A471D/P475D and A471D/P475D/S479D mutants, permitting the pore to host up to six K^+ ions. However, these increments in occupancy were not matched by increases in single-channel conductance, suggesting that the transport rate has already reached its maximum in the P475D variant. Remarkably, additional electrostatic concentrators outside the pore, or traps inside, do not change the ∼200-pS limit for Shaker variants. Thus, conductance in Shaker-type channels is limited by either the translocation across the selectivity filter or by additional steps unrelated to occupancy as, for example, dehydration (unpublished data).

DISCUSSION

Here, we tested the functional dimensions of the intracellular mouth of Shaker-WT and two higher conductance variants having mutations in the PVP region at the internal pore entrance. The neutral variants, Shaker-WT and P475Q, showed similar radii of capture (∼0.82 Å), whereas that of P475D was twofold bigger. We have to keep in mind that these estimates assume that K^+ is a point charge without physical size, and that the pore opening is uncharged. Thus, the actual physical radius would include the effective radius of the permeant ion and its hydration shell (Andersen, 1983). We also tested how channel occupancy influences conductance by measuring g_{max} in Asp variants A471, P475, V476, and S479,

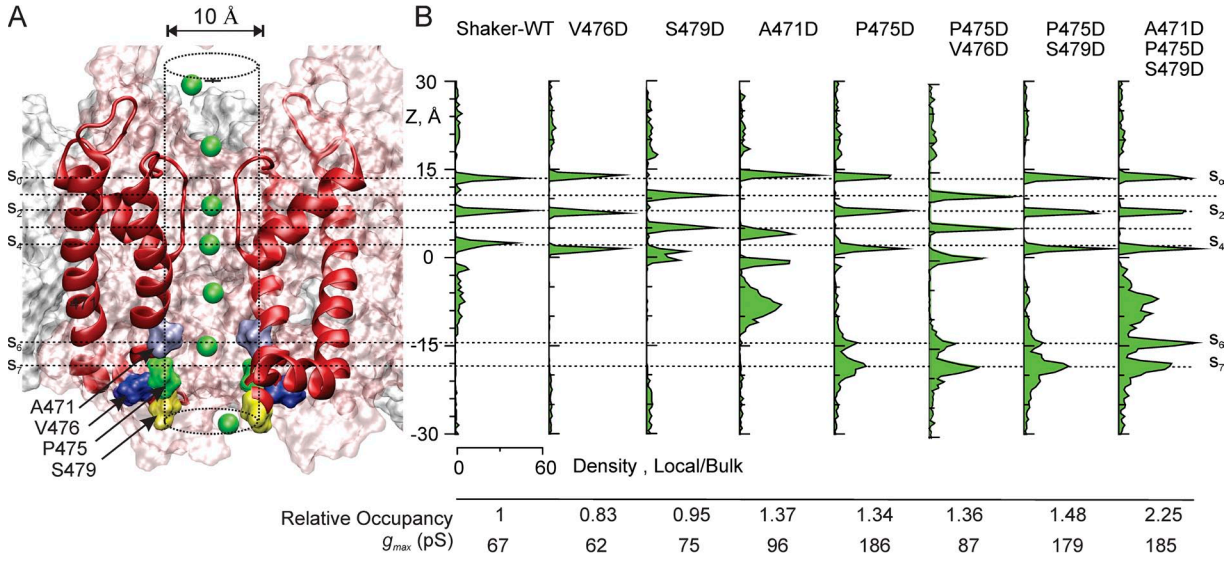

Figure 5. Pore occupancy is modified by charge addition along the permeation pathway. (A) A snapshot of the Shaker pore structure and scheme of occupancy analysis. Shaker protein, shown in light pink, was modeled using the crystallographic structure of Kv1.2 channel as a template (PDB accession no. 2A79; Moscoso et al., 2012). Segments S5–S6, forming the pore domain, are the red ribbons; K^+ are green spheres; lipids are in light gray in surf representation; and residues 471, 475, 476, and 479 are represented as gray, green, blue, and yellow bumps, respectively. The front and back subunits were removed for clarity. The discontinuous lines schematize the 5-Å-radius, pore-concentric cylinder in which time-averaged ion densities were calculated in 0.5-Å-thick slices. (B) Occupancy profile for Shaker-WT, V476D, S479D, A471D, P475D, P475D/V476D, P475D/S479D, and A471D/P475D/S479D calculated by the time-averaged ion densities inside the pore-concentric, 5-Å-radius cylinder relative to the bulk solution (500 mM K^+) during ∼10 ns of simulation. Discontinuous lines indicate the binding sites at z of ∼14, ∼11, ∼8, ∼5, ∼2, approximately −9, approximately −15, and approximately −19 Å for s_0, s_1, s_2, s_3, s_4, s_5, s_6, and s_7, respectively. The drawing in A and B is at approximately the same Z-scale.

being 476D and 479D equivalents to the charged rings in BK channels. In our hands, Shaker-WT unitary conductance increased from ∼25 pS in 100 mM to ∼60 pS in 3,000 mM of symmetric K^+. When added to a WT background, V476D did not increase g_{max}, whereas S479D did by ∼10% and A471D by 50%. On the other hand, when the mutations were added to the high conductance P475D variant (with g_{max} of ∼190 pS), V476D alone halved g_{max}, whereas A471D, S479D, nor A471D/S479D had any effect. Molecular dynamics simulations also indicated that the pore occupancy is indeed increased in all negatively charged mutants. Thus, Shaker maximum unitary conductance appears to have a ceiling near 200 pS, approximately one third of that of BK channels.

Pore dimensions and the hydrated potassium radius

Because P475Q showed similar diffusion-limited currents to those of Shaker-WT, we propose that the Pro→Asp substitution at position 475 did not significantly modify the dimensions of the internal entrance either (Fig. 1). Because in a diffusion-limited regimen the outward unitary current of P475D should be strictly proportional to the potassium concentration, a twofold increment in the P475D diffusion-limited current, with respect to Shaker-WT, suggests that the four Asp carboxyl side chains at position 475 double the K^+ concentration in the vicinity of the intracellular mouth. This twofold increment harmonizes with (a) the observed 50% reduction in the outward current when the internal ionic strength is doubled with NMDG-Cl with respect to equivalent addition of sucrose to parallel the osmolarity change (Moscoso et al., 2012), and (b) the twofold outward currents increment produced by the negatively charged ring in BK and KcsA channels (Brelidze et al., 2003; Nimigean et al., 2003).

Based on diffusion-limited currents, the internal radius of capture (r_c) for K^+ ions in Shaker is ∼0.82 Å, ∼1.4 Å narrower than that of BK channels, with r_c = 2.2 Å (Brelidze and Magleby, 2005). Whether the K^+ ions behave as point charges or solid bodies, these differences should be maintained as long as the geometrical considerations are equally valid for both channel proteins and the diffusional size of K^+ is the same. Although comparisons with the available structural data are warranted, they should be made carefully because of the resulting simplistic geometric assumptions (Läuger, 1976; Andersen, 1983; Hille, 2001; Brelidze and Magleby, 2005). Even worse, the ∼1.4-Å difference in r_C with BK channels requires additional considerations to be taken seriously; for example, it is substantially below the ∼8–10-Å difference between the pore of the large conductance MthK channel and the Kv1.2/2.1 paddle chimera, the template for Shaker channels (radii of ∼12 and ∼5 Å, respectively; Jiang et al., 2002; Long et al., 2007). Moreover, pore dimension of open BK channels could be even larger, as confirmed with double-cysteine modification within the pore (Zhou et al., 2011). Thus, because of these discrepancies around the BK channel structure, here we compare our functional data with the available structural data for Kv channels only. Such comparison allows for an estimate of the effective radius to K^+ ions approaching the channel (see below).

It seems unavoidable to assume that K^+ ions must be hydrated while approaching the internal mouth of the pore. However, the average number of water molecules attached or the effective physical dimensions of the K^+–water complex is much more mysterious. There are several estimations for the average radius of hydrated K^+, ranging between 3 and 6 Å (Enderby, 1995). According to these figures, the diameter of the internal entrance of Shaker should be somewhere between 8 and 14 Å, a number in agreement with the 10–12-Å structural data for Kv1.2 (Long et al., 2005). However, because of the large variation in the estimations of the radius of the hydrated K^+ complex, this approximation remains unsatisfactory.

We approached the dimension of the hydrated K^+ complex entering the pore by calculating the molecular surface of the internal entrance of the channel with a rigid sphere of variable radius rolled on top of van der Waals surface of the exposed residues (Richards, 1977). By taking the difference between the effective pore radius left by the rolling sphere and the radius of the probe (r_P, the radius of the putative hydrated K^+), we obtain an estimation of the capture radius for K^+. When such a difference matches with our diffusion-limited estimates of r_c, the probe becomes an estimation for the hydrodynamic radius of the approaching K^+ ions.

In the VMD environment (Humphrey et al., 1996), we measured the effective pore radius left by the variable radius spherical probe rolled over the surface of the Kv1.2/2.1 paddle chimera crystal structure (PDB accession no. 2R9R; see Materials and methods and Fig. S1). For each probe radius, between 1.3 and 4.5 Å, we drew the largest circumscribed and the smallest inscribed circles in the pore entrance, with radii named r_{max} and r_{min}, respectively (Figs. 6, A–E, and S1, B–E). The effective opening may be somewhere in between these estimates. Because of the loss in surface tortuosity, one expected result in radially symmetric structures is that r_{max} and r_{min} converge to the same value as the probe approaches the pore size. Here, regardless of the size of the probe, the narrowest part of the internal entrance left by the probe always coincided with the side chain of residue 403 (residue 475 in Shaker). To obtain the radius of capture for each probe size, r_P was subtracted to r_{max} ($r_C = r_{max} - r_P$) or to r_{min} ($r_C = r_{min} - r_P$; Fig. 6 F). For probes with a radius >4.5 Å, the effective size of the internal entrance was smaller than the size of the probe, making the passage of the probe cavity geometrically impossible (radius of capture negative). When r_P = 3.8 Å,

the difference $r_C = r_{min} - r_P$ is equal to 0.82 Å, our estimate of the radius of capture. This is a lower limit for the size of a hydrated K^+. Whereas when $r_P = 4.1$ Å, the difference $r_C = r_{max} - r_P$ is 0.82 Å, being the upper limit for the size of a hydrated K^+. These 3.8–4.1-Å estimates are similar to the dimensions of the complex formed by K^+ and its eight water molecules "trapped in flagrante" in the cavity of the KcsA channel, suggesting that K^+ ions approach the pore with one hydration layer tightly bound (Enderby, 1995; Miller, 2001; Zhou et al., 2001). Fig. 6 also makes the structural data harmonize with functional estimates for the internal vestibule diameter attained from the formation of Cd^{2+} cross-bridges in the open pore of Shaker (Webster et al., 2004).

Pore dimensions and the resistance of the permeation pathway

Theoretical calculations across several channel structures showed that most of the voltage profile drops across the selectivity filter; thus, the rate-limiting step for ion conduction should be transitions across this structure (Morais-Cabral et al., 2001; Jiang et al., 2002; Carvacho et al., 2008). These calculations seem to be validated in CNG channels in which voltage-dependent Ag^+ accessibility indicates that ~80% of the field drops across the selectivity filter (Contreras et al., 2010). We have suggested before that the internal cavity of small conductance K and BK channels does not contribute equally to their total channel resistance, being larger in small-conductance channels (Moscoso et al., 2012). In line with this reasoning, our diffusion-limited current experiments on Shaker K channels (Fig. 1) and the effective pore diameter calculations in Fig. 6 on the Kv1.2/2.1 structure from Long et al. (2007) lead us to estimate ~10 Å for the diameter of the internal entrance, narrower than that of BK channels (Brelidze and Magleby, 2005; Zhou et al., 2011). This narrow pore would contribute a higher electrical resistance in small conductance channels, making the electric field significantly drop away from the selectivity filter. These considerations led us to use the decrease in the currents produced by internal/external sucrose to calculate the

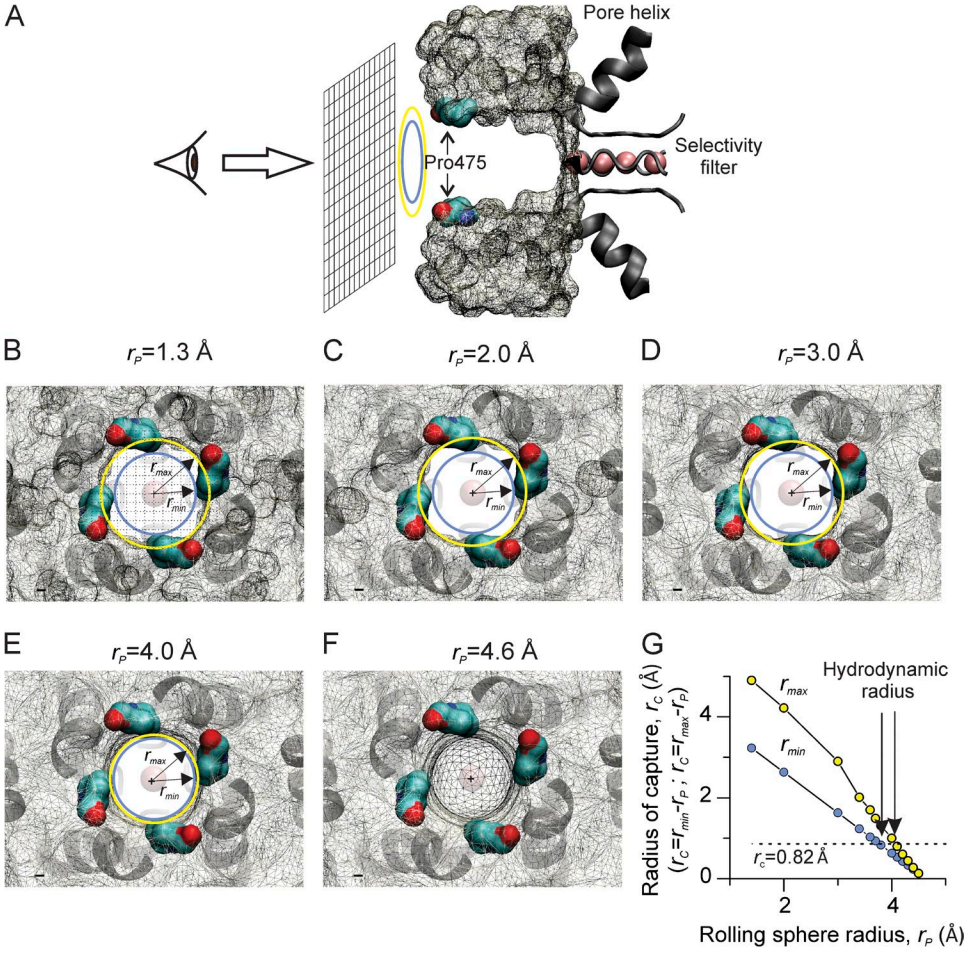

Figure 6. K^+ ion hydrodynamic radius. (A) Schematic lateral view of Kv1.2/2.1 paddle chimera structure (PDB accession no. 2R9R) along the pore. The front and back subunits, together with the voltage sensor and T1 domains, were omitted. A schematic representation of the selectivity filter together with two of the pore helices and two Pro475 residues is shown for reference. Also a scheme of the 1 × 1–Å grid and the circles described by r_{min} and r_{max} are shown in blue and yellow, respectively. The eye and the arrow drawings indicate the point of view for the following images. (B–E) Surfaces left by rolling a sphere of variable radius onto the van der Waals surface of the protein. Radii varied from 1.3 to 4.6 Å (indicated in each panel). For reference, B also shows the 1 × 1–Å grid used to measure the radii r_{min} and r_{max} (represented in blue and yellow, respectively). As the size of the probe increased, the surface left by the probe was less grainy; also, the difference between the two radii decreased. When r_C was ≥4.6 Å (F), the probe was not able to enter the pore. (G) Effective radii of capture, r_C, for r_{min} and r_{max} plotted versus r_P, the radius of the probe. The size of the hydrodynamic radius for K^+ ion was obtained when r_C matched the experimentally obtained capture radius of 0.82 Å (dashed line). The values for the K^+ ion hydrodynamic radius were 3.8 and 4.1 Å for the comparison with the smaller and the bigger circle data, respectively (vertical arrows).

contribution of different sections of the pore to its overall resistance (Figs. 1 and S2, and Table 1). According to our estimations, with at most 3 GΩ, the selectivity filter contributes with <50% of the total pore resistance in the P475D variant. Also, our estimates for the external access resistance are consistent across all variants, giving an overall average of ~1.9 GΩ. On the contrary, the internal access resistances showed much higher variability (Table 1) and were higher than expected from theoretical calculations, suggesting sucrose's partial invasion into the pore (see below). Consider the access resistance, R_{AccIn}, experienced by the ion transiting between some distant point in the bulk of the solution and the internal mouth of the channel approximated by a hemispherical casket shell with radius equal to r_C:

$$R_{AccIn} = \frac{\rho}{2\pi r_C}, \tag{3}$$

where ρ is the resistivity of the 100 mM of KCl solution (120 Ωcm; Hille, 2001, but see Hall, 1975, for a more precise calculation). Assuming an effective r_C of 0.82 Å for Shaker-WT and P475Q, we obtained values of 2.33 GΩ for R_{AccIn}. Meanwhile for P475D, with an effective r_C = 1.6 Å because of the twofold higher diffusion-limited currents (Fig. 1), we obtained R_{AccIn} =1.16 GΩ, in agreement with the experimental estimation of 1.5 GΩ (Table 1). But for the neutral variants, the experimental estimations are approximately fourfold larger than their theoretical counterparts. This discrepancy may indicate that sucrose enters the pore, beyond the access vestibule in the neutral variants, producing an additional increase in their resistance.

To assess the invasion of sucrose into the pore, we could define a partition coefficient for sucrose, or a fraction of the time that sucrose occupies the pore, or simply define two zones within the cavity: one zone more distal, where sucrose has free access and behaves as in the bulk solution; and a second one, deeper into the protein, where sucrose cannot reach. Assuming that sucrose does not change the selectivity filter properties, because it never approaches it, we can divide the total pore electrical resistance, R_T, into five zones (Fig. 7), represented by five in-series resistors:

$$R_T = R_{AccIn} + R_{SucOc} + R_{SucFr} + R_f + R_{AccEx}, \tag{4}$$

where R_f is the resistance of the selectivity filter, which we assume to be sucrose insensitive; R_{SucFr} is the resistance representing the deeper sucrose-inaccessible zone of the cavity (sucrose free); R_{SucOc} is the resistance in the shallower sucrose-accessible zone (sucrose occupied); and R_{AccEx} and R_{AccIn} are the external and internal access resistances, respectively. Then, the total change in channel resistance produced by internal sucrose addition is:

$$R_T^S - R_T = \left(R_{SucOc}^S - R_{SucOc}\right) + \left(R_{AccIn}^S - R_{AccIn}\right), \tag{5}$$

where R_{SucOc}^S and R_{AccIn}^S are the resistances of both sucrose-permissive zones when sucrose is present in the internal solution. Assuming that the resistivity of a 100-mM K^+ solution is 7.14-fold higher after 2 M of sucrose addition (Brelidze and Magleby, 2005), then:

$$R_{SocOc}^S = 7.14 R_{SucOc} \text{ and } R_{AccIn}^S = 7.14 R_{AccIn}.$$

By replacing these expressions in Eq. 5, we obtain: $R_T^S - R_T = 6.14\left(R_{SucOc} + R_{AccIn}\right)$.

For Shaker-WT and P475Q (r_c = 0.82 Å), the calculated R_{AccIn} goes from 2.33 GΩ in control to 17 GΩ with sucrose in the test solution, whereas for P475D, it increased from 1.16 to 8.3 GΩ. In addition, for Shaker-WT, the resistance, measured in the inward currents,

TABLE 2
Sectional resistances along the pore of Shaker variants

Variant	r_C	R_T	R_T^S	R_{AccIn}	R_{AccIn}^S	R_{AccEx}	R_{SucOc}	R_{SucFr}	R_f	$R_{SucFr} + R_f$	%Occ	R_f / R_T
	Å											
WT	0.82	39	90	2.33	16.6	2.1	5.98	25.60	3.0	28.60	0.19	0.08
475Q	0.82	20	77	2.33	16.6	1.5	7.00	6.30	3.0	9.30	0.53	0.15
475D	1.64	6.6	16	1.16	8.30	2.0	0.37	0.07	3.0	3.07	0.84	0.45
BK	4.4[a]	4.0	8.0	0.29	2.07	0.9[b]	0.36	0.45	2.0[c]	2.44	0.45	0.50

Parameters of the in-series connected resistance model. The conduction pathway was divided in five resistors connected in-series (Fig. 7). Resistors are: the external access (R_{AccEx}), measured with Eq. 2; the internal access (R_{AccIn}), calculated from Eq. 3; the sucrose-accessible section (R_{SucOc}); the sucrose-free section (R_{SucFr}); and the selectivity filter (R_f). The capture radius, r_C, is expressed in Å. R_T is the total channel resistance in control, and R_T^S is the total channel resistance after the addition of 2 M sucrose to the internal side. %Occ is the fraction occupied by the sucrose-accessible section, and R_f / R_T is the fraction of the total resistance contributed by the selectivity filter. Values for BK channels were calculated from data in Brelidze and Magleby (2005), who used 150-mM KCl solutions. All resistance values are given in GΩ.

[a]The radius of capture assumes intact charge rings and conductivity of a 150-mM KCl solution.

[b]R_{AccEx} was calculated assuming r_C = 1.4 Å (Yellen, 1984).

[c]R_f was set to two thirds of Shaker's because of the use of 150 mM K^+ instead of 100 mM K^+, and conductance increases nearly linear with K^+ concentration in that range.

changed from 39 to 90 GΩ with sucrose. Then, $R_T^S - R_T = 6.14(R_{SucOc} + 2.3) = 51$ GΩ; thus, $R_{SucOc} = 6.0$ GΩ and then $R_f + R_{SFr}$ is ∼30 GΩ. Because we do not have an estimate for Shaker's R_f, we can assume, based on nearly identical permeability ratio sequences, that it is identical to that of P475D, which is 3.07 GΩ, at the most (Table 1). Assuming that $R_f = 3$ GΩ for all Shaker variants tested here, we estimated the contribution of each zone to the total pore resistance (Table 2). Thus, the cavity resistance ($R_{SucOc} + R_{SucFr}$) in Shaker-WT is ∼32 GΩ, 10-fold larger than that of the selectivity filter, and twice and 70-fold larger than the resistance of P475Q and P475D cavities, respectively.

In WT BK channels, with an intact ring of negative charges, the change in resistance for the inward currents induced by sucrose in 150 mM K^+ is $R_T^S - R_T$ ∼4 GΩ (Brelidze and Magleby, 2005). Taking $r_C = 4.4$ Å as the effective internal radius of capture, then $R_{AccIn} = 0.29$ GΩ. Also, assuming an external radius of capture of 1.4 Å, $R_{AccEx} = 0.91$ GΩ (Yellen, 1984), and using Eq. 4, $R_f + R_{SFr}$ is ∼2.44 GΩ. This figure set an upper limit for BK channels' R_f that, because it is comparable to the total pore resistance, is consistent with a highly focused electric field across this structure (Jiang et al., 2002; Jogini and Roux, 2005). Thus, assuming $R_f = 2$ GΩ (because BK channel measurements were made in 150 mM K^+), ∼50% of the voltage would drop across its selectivity filter, whereas only 8% would do it across Shaker's. Thus, BK channel cavity resistance is ∼0.8 GΩ, ∼1/44 of that of Shaker's cavity.

Geng et al. (2011) measured the resistance changes of part of the entrance pathway of BK channels' inner cavity, delimited by the charged rings at positions 321 and 324, whose volume was altered when amino acid side chains were changed. These experimental maneuvers may have also altered the access resistance, but the authors did not explicitly state it. When mapped on the structure of the open MthK channel, this slice corresponded to approximately one third of the inner cavity volume. If we assume, according to our model applied to the data from Brelidze and Magleby (2005), that BK channels' cavity resistance is 0.81 GΩ, then the slice resistance should be $(R_{SucOc} + R_{SucFr})/3 + R_{AccIn} = 0.56$ GΩ. This value is in reasonably good agreement with the 0.34–0.45 GΩ estimated by Geng et al. (2011), considering the differences in the experimental and methodological approaches.

Translating these resistances ratios between Shaker and BK channel cavities to the energy that the ions require to go across the pore, 1/40 in the rate of ion transport is equivalent to ∼2.2 kcal mol^{-1}. This energy difference could be caused by the dissimilarities in the physical dimensions of each pore. The free energy of an ion inside the center of a cylindrical aqueous cavity decreases by 1.5–28 kcal mol^{-1} $Å^{-1}$ in radius (Parsegian, 1969; Chung et al., 2002; Jogini and Roux, 2005; Treptow and Tarek, 2006). Thus, if we extend the ∼1.4-Å difference in their capture radius to the whole cavity, assuming cylindrical geometries, on average a K^+ ion would be ∼40-fold more comfortable in the BK channel wider cavity. Keeping in mind the architectural and chemical complexities of each channel, this analogy could be a large oversimplification; however, the trend relating the energy with the cavity dimensions is not only theoretically supported (Parsegian, 1969) but also accurate in representing the attributes of several ion channels (Jogini and Roux, 2005; Treptow and Tarek, 2006). Thus, a narrower cavity, where ions interact more intimately with the channel walls, would exhibit a resistance increment much larger than that expected solely by reducing the cross-sectional area for diffusion.

Alternatively, friction with the pore walls could also make ions go slower. Let's imagine a K^+ ion with its squared antiprism water cage rolling around the narrow Shaker pore (Zhou et al., 2001). If rigid, the cage would be bouncing with every little bump in the pore walls. On the other hand, in a wide cavity, the water molecules of the second (and loosely bound) hydration shell would act as "ball-bearing" sliding mechanisms, reducing the effective friction of the cage. To our knowledge, this possibility has not been tested seriously for ion diffusion in narrow pores; however, in this regard, it is interesting that the difference in the capture diameters ($2 \times r_C$) between BK and Shaker channels is ∼2.8 Å,

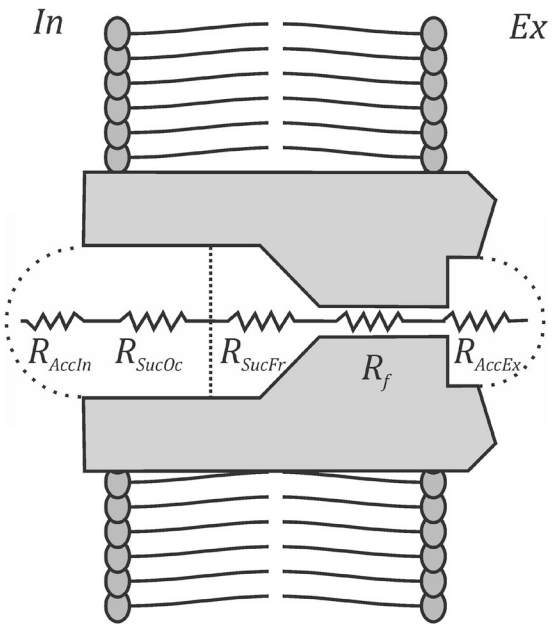

Figure 7. In-series connected resistance model. The conduction pathway was divided into five resistors connected in-series: the external and internal access resistances, R_{AccIn} and R_{AccEx}, respectively; the resistance of the section occupied by sucrose, R_{SucOc}; the resistance of the sucrose-free section, R_{SucFr}; and the selectivity filter, R_f. See Table 2 for details of resistance calculations.

the size of a water molecule. Thus, there is enough space for "ball-bearing sliding."

We have proposed a common experimentally derived parameter, the sectional electrical resistance, to account for the diversity in single-channel conductances despite the high conservation in the selectivity filter structure among the potassium channel superfamily. In this scheme, the diverse unitary conductances reside in the cavity's contribution to the total resistance. The low conductance of Shaker channels could be caused by: (a) the high resistance associated with the energetic cost of placing a cation in its narrower aqueous cavity immersed in a low dielectric, or (b) to a higher friction delivered by a rigid hydration cage bumping with cavity walls. Charge addition to the Shaker cavity made it more ion friendly and reduced its resistance. Table 2 shows that the P475D cavity resistance is ∼1/70 that of Shaker-WT, reaching a value comparable to that of BK channels. Thus, within this perspective, the addition of negative charges to the cavity circumvents the excess energy required to introduce an ion in it. The negative charge additions to the conduction pathway increased significantly the pore occupancy but did not increase maximum unitary conductance beyond the ∼200-pS ceiling (Figs. 3 and 4). This limit indicates the existence of additional barriers or steps for K^+ permeation to overcome in Shaker-type channels in order to match BK channels. These barriers could be, for example, friction, dehydration step(s) to enter/exit the selectivity filter, or simply threefold slower translocation across the selectivity filter, which in activation energy terms is equivalent to ∼1 kT.

We thank Ramón Latorre and Bill Griesar (WSU-Vancouver and http://nwnoggin.org) for critical reading of the manuscript, to the Galvani group for suggestions, and to Lorena Prado and Vicky Prado for excellent technical help.

This work was supported by Fondecyt grants 1120819 and 1131003, and by ACT1107 and ICM-P09-022-F. I. Díaz-Franulic and R. Sepúlveda are Mecesup and Conicyt-2113063 doctoral fellows, respectively. The Centro Interdisciplinario de Neurociencia de Valparaíso is a Millennium Institute supported by the Millennium Scientific Initiative of the Ministerio de Economía, Fomento y Turismo.

The authors declare no competing financial interests.

Kenton J. Swartz served as editor.

Submitted: 30 December 2014
Accepted: 2 June 2015

REFERENCES

Andersen, O.S. 1983. Ion movement through gramicidin A channels. Studies on the diffusion-controlled association step. *Biophys. J.* 41:147–165. http://dx.doi.org/10.1016/S0006-3495(83)84416-6

Andersen, O.S., and J. Procopio. 1980. Ion movement through gramicidin A channels. On the importance of the aqueous diffusion resistance and ion-water interactions. *Acta Physiol. Scand. Suppl.* 481:27–35.

Bezanilla, F., and C.M. Armstrong. 1972. Negative conductance caused by entry of sodium and cesium ions into the potassium channels of squid axons. *J. Gen. Physiol.* 60:588–608. http://dx.doi.org/10.1085/jgp.60.5.588

Blatz, A.L., and K.L. Magleby. 1986. Single apamin-blocked Ca-activated K^+ channels of small conductance in cultured rat skeletal muscle. *Nature.* 323:718–720. http://dx.doi.org/10.1038/323718a0

Brelidze, T.I., and K.L. Magleby. 2005. Probing the geometry of the inner vestibule of BK channels with sugars. *J. Gen. Physiol.* 126:105–121. http://dx.doi.org/10.1085/jgp.200509286

Brelidze, T.I., X. Niu, and K.L. Magleby. 2003. A ring of eight conserved negatively charged amino acids doubles the conductance of BK channels and prevents inward rectification. *Proc. Natl. Acad. Sci. USA.* 100:9017–9022. http://dx.doi.org/10.1073/pnas.1532257100

Carvacho, I., W. Gonzalez, Y.P. Torres, S. Brauchi, O. Alvarez, F.D. Gonzalez-Nilo, and R. Latorre. 2008. Intrinsic electrostatic potential in the BK channel pore: Role in determining single channel conductance and block. *J. Gen. Physiol.* 131:147–161. http://dx.doi.org/10.1085/jgp.200709862

Chung, S.H., T.W. Allen, and S. Kuyucak. 2002. Conducting-state properties of the KcsA potassium channel from molecular and Brownian dynamics simulations. *Biophys. J.* 82:628–645. http://dx.doi.org/10.1016/S0006-3495(02)75427-1

Contreras, J.E., J. Chen, A.Y. Lau, V. Jogini, B. Roux, and M. Holmgren. 2010. Voltage profile along the permeation pathway of an open channel. *Biophys. J.* 99:2863–2869. http://dx.doi.org/10.1016/j.bpj.2010.08.053

Eisenman, G., R. Latorre, and C. Miller. 1986. Multi-ion conduction and selectivity in the high-conductance Ca^{++}-activated K^+ channel from skeletal muscle. *Biophys. J.* 50:1025–1034. http://dx.doi.org/10.1016/S0006-3495(86)83546-9

Enderby, J.E. 1995. Ion solvation via neutron scattering. *Chem. Soc. Rev.* 24:159–168. http://dx.doi.org/10.1039/cs9952400159

Feller, S.E., Y. Zhang, R.W. Pastor, and B.R. Brooks. 1995. Constant pressure molecular dynamics simulation: The Langevin piston method. *J. Chem. Phys.* 103:4613–4621. http://dx.doi.org/10.1063/1.470648

Ferry, J.D. 1936. Statistical evaluation of sieve constants in ultrafiltration. *J. Gen. Physiol.* 20:95–104. http://dx.doi.org/10.1085/jgp.20.1.95

Geng, Y., X. Niu, and K.L. Magleby. 2011. Low resistance, large dimension entrance to the inner cavity of BK channels determined by changing side-chain volume. *J. Gen. Physiol.* 137:533–548.

Hackos, D.H., T.H. Chang, and K.J. Swartz. 2002. Scanning the intracellular S6 activation gate in the shaker K^+ channel. *J. Gen. Physiol.* 119:521–532. http://dx.doi.org/10.1085/jgp.20028569

Hall, J.E. 1975. Access resistance of a small circular pore. *J. Gen. Physiol.* 66:531–532. http://dx.doi.org/10.1085/jgp.66.4.531

Harris, R.E., H.P. Larsson, and E.Y. Isacoff. 1998. A permanent ion binding site located between two gates of the Shaker K^+ channel. *Biophys. J.* 74:1808–1820. http://dx.doi.org/10.1016/S0006-3495(98)77891-9

Heginbotham, L., and R. MacKinnon. 1993. Conduction properties of the cloned Shaker K^+ channel. *Biophys. J.* 65:2089–2096. http://dx.doi.org/10.1016/S0006-3495(93)81244-X

Heginbotham, L., Z. Lu, T. Abramson, and R. MacKinnon. 1994. Mutations in the K^+ channel signature sequence. *Biophys. J.* 66:1061–1067. http://dx.doi.org/10.1016/S0006-3495(94)80887-2

Hénin, J., W. Shinoda, and M.L. Klein. 2008. United-atom acyl chains for CHARMM phospholipids. *J. Phys. Chem. B.* 112:7008–7015. http://dx.doi.org/10.1021/jp800687p

Hille, B. 2001. Ion Channels of Excitable Membranes. Third edition. Sinauer, Sunderland, MA. 814 pp.

Humphrey, W., A. Dalke, and K. Schulten. 1996. VMD: visual molecular dynamics. *J. Mol. Graph.* 14:33–38. http://dx.doi.org/10.1016/0263-7855(96)00018-5

Jiang, Y., A. Lee, J. Chen, M. Cadene, B.T. Chait, and R. MacKinnon. 2002. The open pore conformation of potassium channels. *Nature.* 417:523–526. http://dx.doi.org/10.1038/417523a

Jogini, V., and B. Roux. 2005. Electrostatics of the intracellular vestibule of K^+ channels. *J. Mol. Biol.* 354:272–288. http://dx.doi.org/10.1016/j.jmb.2005.09.031

Jorgensen, W.L., J. Chandrasekhar, J.D. Madura, R.W. Impey, and M.L. Klein. 1983. Comparison of simple potential functions for simulating liquid water. *J. Chem. Phys.* 79:926–935. http://dx.doi.org/10.1063/1.445869

Latorre, R., and C. Miller. 1983. Conduction and selectivity in potassium channels. *J. Membr. Biol.* 71:11–30. http://dx.doi.org/10.1007/BF01870671

Läuger, P. 1976. Diffusion-limited ion flow through pores. *Biochim. Biophys. Acta.* 455:493–509. http://dx.doi.org/10.1016/0005-2736(76)90320-5

Long, S.B., E.B. Campbell, and R. Mackinnon. 2005. Crystal structure of a mammalian voltage-dependent Shaker family K^+ channel. *Science.* 309:897–903. http://dx.doi.org/10.1126/science.1116269

Long, S.B., X. Tao, E.B. Campbell, and R. MacKinnon. 2007. Atomic structure of a voltage-dependent K^+ channel in a lipid membrane-like environment. *Nature.* 450:376–382. http://dx.doi.org/10.1038/nature06265

MacKerell, A.D., Jr., D. Bashford, M. Bellott, R.L. Dunbrack, J.D. Evanseck, M.J. Field, S. Fischer, J. Gao, H. Guo, S. Ha, et al. 1998. All-atom empirical potential for molecular modeling and dynamics studies of proteins. *J. Phys. Chem. B.* 102:3586–3616. http://dx.doi.org/10.1021/jp973084f

Mackerell, A.D., Jr., M. Feig, and C.L. Brooks III. 2004. Extending the treatment of backbone energetics in protein force fields: Limitations of gas-phase quantum mechanics in reproducing protein conformational distributions in molecular dynamics simulations. *J. Comput. Chem.* 25:1400–1415. http://dx.doi.org/10.1002/jcc.20065

MacKinnon, R., and C. Miller. 1989. Functional modification of calcium-activated potassium channel by trimethyloxonium. *Biochemistry.* 28:8087–8092. http://dx.doi.org/10.1021/bi00446a019

Miller, C. 2001. See potassium run. *Nature.* 414:23–24. http://dx.doi.org/10.1038/35102126

Morais-Cabral, J.H., Y. Zhou, and R. MacKinnon. 2001. Energetic optimization of ion conduction rate by the K^+ selectivity filter. *Nature.* 414:37–42. http://dx.doi.org/10.1038/35102000

Moscoso, C., A. Vergara-Jaque, V. Márquez-Miranda, R.V. Sepúlveda, I. Valencia, I. Díaz-Franulic, F. González-Nilo, and D. Naranjo. 2012. K^+ conduction and Mg^{2+} blockade in a shaker Kv-channel single point mutant with an unusually high conductance. *Biophys. J.* 103:1198–1207. http://dx.doi.org/10.1016/j.bpj.2012.08.015

Naranjo, D., and R. Latorre. 1993. Ion conduction in substates of the batrachotoxin-modified Na^+ channel from toad skeletal muscle. *Biophys. J.* 64:1038–1050. http://dx.doi.org/10.1016/S0006-3495(93)81469-3

Nimigean, C.M., J.S. Chappie, and C. Miller. 2003. Electrostatic tuning of ion conductance in potassium channels. *Biochemistry.* 42:9263–9268. http://dx.doi.org/10.1021/bi0348720

Parsegian, A. 1969. Energy of an ion crossing a low dielectric membrane: Solutions to four relevant electrostatic problems. *Nature.* 221:844–846. http://dx.doi.org/10.1038/221844a0

Phillips, J.C., R. Braun, W. Wang, J. Gumbart, E. Tajkhorshid, E. Villa, C. Chipot, R.D. Skeel, L. Kalé, and K. Schulten. 2005. Scalable molecular dynamics with NAMD. *J. Comput. Chem.* 26:1781–1802. http://dx.doi.org/10.1002/jcc.20289

Richards, F.M. 1977. Areas, volumes, packing and protein structure. *Annu. Rev. Biophys. Bioeng.* 6:151–176. http://dx.doi.org/10.1146/annurev.bb.06.060177.001055

Sukhareva, M., D.H. Hackos, and K.J. Swartz. 2003. Constitutive activation of the Shaker Kv channel. *J. Gen. Physiol.* 122:541–556. http://dx.doi.org/10.1085/jgp.200308905

Treptow, W., and M. Tarek. 2006. Molecular restraints in the permeation pathway of ion channels. *Biophys. J.* 91:L26–L28. http://dx.doi.org/10.1529/biophysj.106.087437

Webster, S.M., D. Del Camino, J.P. Dekker, and G. Yellen. 2004. Intracellular gate opening in Shaker K^+ channels defined by high-affinity metal bridges. *Nature.* 428:864–868. http://dx.doi.org/10.1038/nature02468

Wilman, H.R., J. Shi, and C.M. Deane. 2014. Helix kinks are equally prevalent in soluble and membrane proteins. *Proteins.* 82:1960–1970. http://dx.doi.org/10.1002/prot.24550

Yellen, G. 1984. Ionic permeation and blockade in Ca^{2+}-activated K^+ channels of bovine chromaffin cells. *J. Gen. Physiol.* 84:157–186. http://dx.doi.org/10.1085/jgp.84.2.157

Yu, H., S.Y. Noskov, and B. Roux. 2010. Two mechanisms of ion selectivity in protein binding sites. *Proc. Natl. Acad. Sci. USA.* 107:20329–20334. http://dx.doi.org/10.1073/pnas.1007150107

Zhou, Y., J.H. Morais-Cabral, A. Kaufman, and R. MacKinnon. 2001. Chemistry of ion coordination and hydration revealed by a K^+ channel-Fab complex at 2.0 Å resolution. *Nature.* 414:43–48. http://dx.doi.org/10.1038/35102009

Zhou, Y., X.M. Xia, and C.J. Lingle. 2011. Cysteine scanning and modification reveal major differences between BK channels and Kv channels in the inner pore region. *Proc. Natl. Acad. Sci. USA.* 108:12161–12166. http://dx.doi.org/10.1073/pnas.1104150108